Continuous and discrete modeling of the decay of two-dimensional nanostructures

2009 J. Phys.: Condens. Matter 21 263001

(http://iopscience.iop.org/0953-8984/21/26/263001)

IOP Publishing Journal of Physics: Condensed Matter

J. Phys.: Condens. Matter **21** (2009) 263001 (12pp) doi:10.1088/0953-8984/21/26/263001

TOPICAL REVIEW

Continuous and discrete modeling of the decay of two-dimensional nanostructures

Marcos F Castez and Ezequiel V Albano

Instituto de Investigaciones Fisicoquímicas Teóricas y Aplicadas (INIFTA), CCT La Plata, Casilla de Correo 16, Sucursal 4, (1900) La Plata, UNLP, CONICET, Argentina

Received 10 November 2008
Published 27 May 2009
Online at stacks.iop.org/JPhysCM/21/263001

Abstract

In this work we review some recent research on the surface diffusion-mediated decay of two-dimensional nanostructures. These results include both a continuous, vectorial model and a discrete kinetic Monte Carlo approach. Predictions from the standard linear continuous theory of surface-diffusion-driven interface decay are contrasted with simulational results both from kinetic and morphological points of view. In particular, we focused our attention on high-aspect-ratio nanostructures, where strong deviations from linear theory take place, including nonexponential amplitude decay and the emergence of several interesting nanostructures such as overhangs developing, nanoislands and nanovoids formation, loss of convexity, nanostructures-pinch off and nanostructures-break off, etc.

(Some figures in this article are in colour only in the electronic version)

Contents

1. Introduction 1
2. The linear theory of surface-diffusion-driven interface decay 2
3. Continuous modeling 2
4. Kinetic Monte Carlo modeling 4
5. Summary and concluding remarks 8
Acknowledgments 11
References 11

1. Introduction

The study of the dynamic and the morphological stability of structured surfaces, and in particular nanostructures evolving by surface diffusion currents, has attracted a great interest during recent years, both from the theoretical and the experimental points of view [1–16]. In fact, such a study is closely related to topics of great relevance in emerging nanotechnology, such as the design of new methods in nanofabrication [17, 18] or the problem of nanostructure stability [19]. The understanding of the processes involved has great technological importance, because it is useful not only for the development of nanofabrication mechanisms [20], but also for tracking the problem of the stability of nanostructures. In fact, current technologies allow us to achieve a high degree of control on superficial nanostructures, e.g. modern techniques can be used to grow specific nanostructures resolved at the atomic scale [18]. Nevertheless, such capabilities in nanofabrication must confront the fact that the obtained structures are often unstable, strongly limiting the field of possible applications. Moreover, structured surfaces play a major role in modern technologies, thus attracting the attention of the research community from theoretical physicists to materials scientists. The reason for this ever-growing interest lies on the wide range of technological applications of structured surfaces, including solar cells, distributed feedback lasers or microelectromechanical systems.

Surface diffusion currents can be useful to change shapes in the nanoworld, e.g. by using a thermal treatment capable of improving a given nanostructure [20]. That would certainly be a 'desirable' consequence of surface diffusion currents. Nevertheless, surface diffusion currents can bring about 'undesirable' effects, such as, for example, if a given built nanostructure becomes thermally unstable and decays in macroscopically short times. Within this context, a broad knowledge on the dynamic and morphological properties of nanostructure evolution driven by surface diffusion currents becomes necessary in order to develop strategies capable

of enhancing the 'positive aspects' of surface diffusion, or, in more specific words, controlling these physical processes for a given nanotechnological application. It is expected that the spread of experimental techniques that allow greater control of materials at the nanoscale and the release of more powerful computers will lead to a deeper comparison between experiments and computer simulations in the near future, further stimulating the interest in surface science at the nanoscale.

Within this broad scenario, in this work we review some recent theoretical advances on the evolution of two-dimensional nanostructures driven by surface diffusion currents [21–24]. Such results are mainly referred to both the continuous and discrete modeling of the decay of high-aspect-ratio interfaces. For such interfaces the small-slopes approximation does not hold and, in consequence, linear theory of surface diffusion is not a good description of interface evolution. The rest of this review is organized as follows. In section 2 we describe the fundamental results of the linear theory of surface diffusion. In section 3 we review the most important kinetic and morphological results obtained in the continuous modeling of surface diffusion in cases far from the small-slopes approximation. Discrete kinetic Monte Carlo models used for the description of those phenomena are discussed in section 4. Finally, in section 5 we present a summary and the concluding remarks.

2. The linear theory of surface-diffusion-driven interface decay

Continuous theory of interface evolution mediated by surface diffusion is a well-established topic dating back to work by Mullins [25, 26] and Herring [27, 28]. One of the key contributions from their work is the understanding of the relationship between surface diffusion currents and a geometrical property of the surface: the local curvature. In fact, within this mesoscopic approach the surface diffusion flux is proportional to the gradient of the local curvature. Of course, in the derivation of such dependence, there is not only an implicit assumption of smoothness for the surface, as is required by a proper definition of curvature, but also an underlying local equilibrium hypothesis to have well-defined thermodynamical coefficients such as surface tension. The underlying hypothesis of smoothness in thermodynamical quantities such as the surface tension leads to the broadly accepted belief that the applicability of this approach would be restricted to temperatures above the roughening temperature T_R [29], since it is known that the surface tension is discontinuous for temperatures below T_R.

As was pointed out by Mullins in his seminal work on thermal grooving on boundary grains [25], normal velocity v_n for a surface element along its normal is given by

$$v_n = -\frac{D_s \gamma \Omega^2 \nu}{k_B T} \frac{\partial^2 \mathcal{C}}{\partial s^2}, \tag{1}$$

where D_s is the surface diffusion constant, $\mathcal{C}$ the local curvature, s the arc length parameter along the interface, γ the surface free-energy per unit area (unit length in the 2D case), Ω the molecular volume ('molecular area' in the 2D case), ν the number of atoms per unit area (unit length in the 2D case), k_B the Boltzmann constant, and T the absolute temperature.

The surface diffusion flow defined by the equation (1) is conservative, which means that the total surface (total volume in the 3D case) remains constant. Moreover, under a certain hypothesis concerning the smoothness of the initial condition, it can be proved that this surface diffusion flow makes the total length (total area in the 3D case) to decrease [30].

Already in the pioneering work by Mullins, most attention has been drawn to the case of interfaces in the small-slope approximation (this was mostly due to the resultant simplicity of the equations rather than to physical motivations). Subsequently, also a great deal of attention in the related literature was focused on the following equation, directly obtained by applying Mullins's ideas in the small-slope case [31–34]

$$\frac{\partial h(x,t)}{\partial t} = -K \frac{\partial^4 h}{\partial x^4}, \tag{2}$$

where h is a single-valued function that describes the interface and K is given by

$$K = \frac{D_s \gamma \Omega^2 \nu}{k_B T}. \tag{3}$$

By a direct substitution into the linear equation (2), we can see that at time t, a Fourier mode of the initial interface $A \sin(kx)$ evolves into

$$h(x,t) = A \exp(-Kk^4 t) \sin\left(kx\right). \tag{4}$$

Equation (4) is an interesting result since it shows that every Fourier mode performs an exponential decay whose lifetime depends on temperature through the constant K and on the wavelength λ. In fact, equation (4) shows that the decay constant, in this small-slope case, is proportional to λ^{-4}, i.e. under the small-slopes approximation, the linear theory predicts a fast filtering of high-frequency features of a given interface. From the morphologic point of view, linear theory, as established by equation (4), predicts that a sinusoidal pattern evolves in a sinusoidal pattern with smaller amplitude. Thus we can say that a single Fourier mode evolves in a shape-preserving way.

3. Continuous modeling

The general case in which interfaces are not under the small-slope approximation has been considered in some detail in a recent paper [22], in which a vectorial, stochastic difference equation for the evolution of two-dimensional interfaces has been studied in a more general context. Let us consider only the deterministic evolution of the model described in [22], in the absence of incident flow (i.e. surface diffusion as the only relevant process). Under this restriction, such a difference equation is

$$\delta\vec{r}(s,t) = -K \frac{\partial^2 \mathcal{C}}{\partial s^2} \, \mathrm{d}t \vec{n} \tag{5}$$

where $\delta\vec{r}(s,t)$ is the local update of the interface when time is advanced in $\mathrm{d}t$ and $\vec{n}$ is the local unitary outward normal

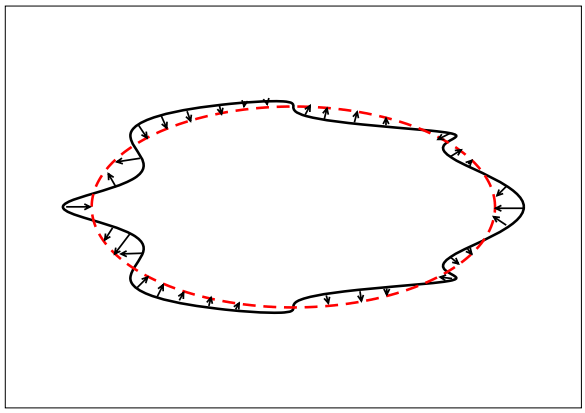

Figure 1. (Color online) Schematic view of the evolution of the interface following the normal vector according to equation (5), where surface diffusion currents are proportional to the local curvature gradient.

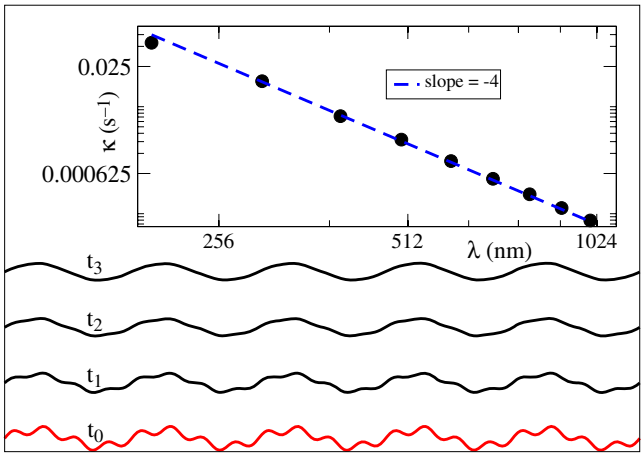

Figure 2. (Color online) An initial interface composed by a linear combination of Fourier modes with wavelengths λ and 2λ evolving with equation (5). At successive steps $t_0 < t_1 < t_2 < t_3$ the filtering of the highest-frequency mode (that one with wavelength λ) occurs, in agreement with the linear theory prediction (4). Inset: log–log plot of the decaying constant κ as a function of the wavelength λ.

vector. Evolution proceeds in a Huygens' construction fashion, familiar from classical optics [35], sketched in figure 1.

Equation (5) is not restricted to small slopes as its linear counterpart given by (2) is. Moreover a numerical integration of the equation (5) [22] shows that it recovers the linear theory predictions when it is applied to initial interfaces that satisfy the small-slopes approximation. In fact, we can see in figure 2 how fast filtering of high-spatial-frequency modes takes place when the initial interface is a linear combination of two small-amplitude sine waves with wavelengths λ and 2λ. After a certain period of time, only the component with larger wavelength (λ) survives. The observed amplitude decay is exponential, in complete agreement with the linear theory prediction (4). In particular (see the inset in figure 2), the decaying constant κ has a power-law dependence on the wavelength: $\kappa \propto \lambda^{-4}$.

It is worth mentioning that these characteristics facts of the linear theory, namely exponential decay of interface features

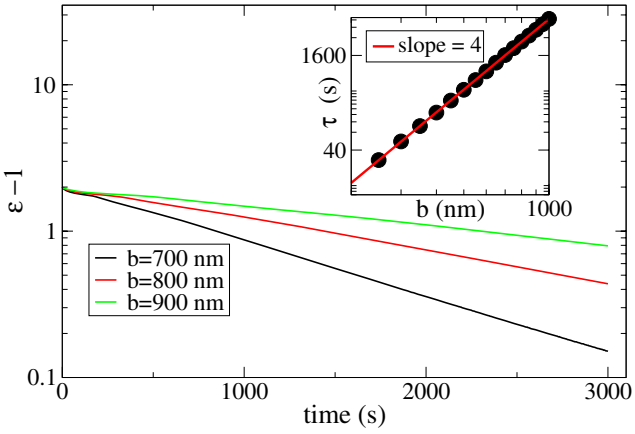

Figure 3. (Color online) Dependence of the aspect ratio $\epsilon - 1$ against time for initial elliptical interfaces with semiaxes a and b. The log–linear scale reveals a nearly exponential decay whose lifetime grows with b^4 (see inset).

and the power-law dependence of the characteristic timescales against the fourth power of λ, are not restricted to the decay of single Fourier modes. In fact, these aspects can be recovered by considering very different situations. For instance, let us consider the evolution of a plane ellipse with semiaxes a and b. The conservative nature of surface diffusion implies that asymptotically the ellipse turns out into a circle [22] (constant curvature curve with smaller length for a given enclosed area) with the same area than the original ellipse. If we consider the aspect-ratio ϵ of the evolving curve, this reasoning leads us to expect that $\epsilon \to 1$ for a long enough time. In figure 3 we have plotted the time evolution of $\epsilon - 1$ showing that, after a short transient, an exponential decay is found. Moreover, the lifetime (let us call τ the lifetime) dependence on λ is given again through the relationship $\tau \propto \lambda^4$, as is shown in the inset of figure 3.

When the aspect ratio of the initial interface departs from the small-slope approximation, strong deviations from linear theory expectations can be observed. This can be observed if we consider the decay of sinusoidal interfaces: while linear theory predicts a shape-preserving decay according to equation (4) if we consider the decay of sinusoidal interfaces with initial aspect ratios of the order of 1, a completely different scheme is found if the interface evolves according to equation (5). In fact, the evolution is no longer shape-preserving and, in particular, there is a transient stage that exhibits a new morphological behavior, because the initially sinusoidal interface develops overhangs spontaneously, recovering the sinusoidal shape at the final stage of the evolution. The different stages in the surface diffusion-mediated decaying of high-amplitude sine-like patterns are outlined in figure 4. Moreover, as has been pointed out in [23], the actual evolution of an initially sine-like pattern with initial aspect ratio in the order of 1 (i.e., far from the small-slope approximation) can very closely be approximated by the following vectorial parametric equation:

$$\vec{r}(p,t) = \left(p - B(t)\sin\left(\frac{4\pi p}{\lambda}\right), A(t)\sin\left(\frac{2\pi p}{\lambda}\right)\right), \quad (6)$$

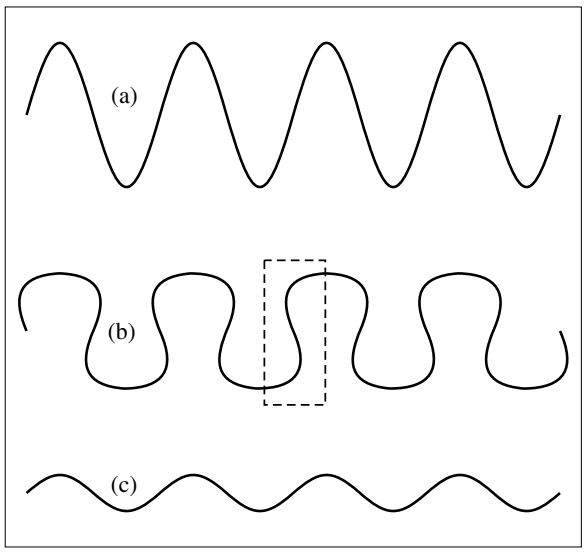

Figure 4. Schematic view of the decay of sine waves driven by (curvature-dependent) surface diffusion currents in dimension 1+1. In (a) the initial profile, a sine wave far from the small-slope approximation, is shown. (b) represents the transient regime in which the interface develops spontaneously overhangs (as is stressed in the dashed box) and departs from the sine-like shape. Finally, in the late evolution stage, the interface recovers the sine-like shape with a smaller amplitude, as is shown in (c).

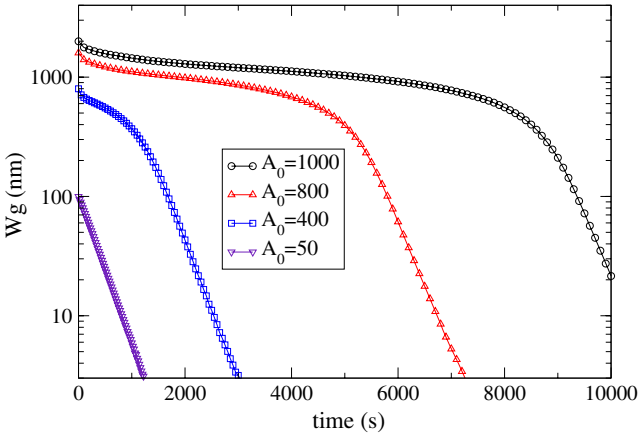

Figure 5. (Color online) Log–linear plots of the global width, defined as the difference between the interface global maximum and minimum, as a function of time. Results obtained by a numerical integration of equation (5) with an initially sinusoidal interface (with $\lambda = 1000$ nm and $K = 1.8610^6$ nm^{4}s^{-1}) for several initial amplitudes (as listed in the figure in units of nm). The departure from the pure exponential decay mode becomes evident, within the short-time regime, when initial amplitudes are increased, and the initial conditions of the interface lie far from the small-slope case.

where $\vec{r}$ is a vectorial function whose value, at a fixed time t, depends only on the parameter p, while $A(t)$ and $B(t)$ are coefficients to be fitted from the numerical data.

Differences between the linear theory of surface diffusion and that predicted by the general equation (5) are not restricted to morphological aspects. In fact, according to equation (4) the linear theory predicts an exponential decay of the global width W_g (defined as the difference between the interface global maximum and minimum) as a function of time. The time evolution of W_g according to equation (5) is shown in figure 5, where we can see a different relaxation behavior for the decay of initially sinusoidal interfaces of the same wavelength ($\lambda = 1000$ nm): while by starting from small amplitudes, the global width W_g decays exponentially with time, a nonexponential transient takes place when the initial interface is far from the small-slope approximation. As was discussed in [22], this nonexponential decay occurs simultaneously with the spontaneous formation of overhangs.

4. Kinetic Monte Carlo modeling

Let us consider a two-dimensional triangular lattice of sides $L_x \times L_y$ on which particles (atoms or molecules) can diffuse. Each site of the lattice can be in one of two possible states: occupied (by a particle) or empty. We shall introduce the occupation number n_{ij} that takes the value 1 if the site (i, j) is occupied and 0 if the site (i, j) is empty. A periodic boundary condition is imposed on the lattice along the x direction, while a free boundary condition is imposed along the y direction by introducing two extra rows in the lattice, corresponding to $j = 0$ and $L_y + 1$, which we shall call the *bottom* and the *top* of the system, respectively. Such extra rows cannot be occupied by particles, and sites on these rows will be called 'forbidden sites'. We shall assume that every particle on the lattice interacts with its neighbors through the following Hamiltonian:

$$H = E_b \sum_{\langle i,j,l,m \rangle} n_{ij} n_{lm} + 2E_b \sum_{i=1}^{L_x} n_{i1}, \qquad (7)$$

where $\langle\,\rangle$ denotes a nearest-neighbor restricted summation and E_b is the bond energy between two nearest-neighbor particles. In this way, the first summation corresponds to bulk interactions among particles, while the second one accounts for the interaction between particles and the bottom wall.

In a single diffusion event a particle in the (i, j) position $(1 \leqslant i \leqslant L_x, 1 \leqslant j \leqslant L_y)$ of such a lattice can jump into one of its six neighboring sites, provided that such a site is empty, and, since surface diffusion is the only process considered by the model, the dynamics of the system is conservative and the total number of particles N_T is constant during the whole evolution.

Diffusion processes have been implemented under the KMC approach, with transition rates evaluated according to the harmonic transition state theory, i.e. the transition rate for a transition from configuration c_{ini} to configuration c_{fin} is given by

$$W(c_{ini} \to c_{fin}) = \nu_0 \exp\big[-E^{act}(c_{ini}, c_{fin})/k_B T\big], \qquad (8)$$

where ν_0 is the effective vibration frequency, $E^{act}(c_{ini}, c_{fin})$ is the activation energy for a transition between c_{ini} and c_{fin}. Throughout this work, we have take $\nu_0 = 5 \times 10^{12}$ Hz. As was pointed by Weinberg and co-workers [36–38], the kind of dynamics that induces the transition rate given by equation (8) satisfies the detailed balance condition for

a Boltzmannian equilibrium state as the standard dynamic rules, such as Kawasaki, Glauber or Metropolis dynamics do [39–42]. Also, $W(c_{\rm ini} \rightarrow c_{\rm fin})$ represents a physical quantity since it is proportional to the probability of success for thermally activated barrier crossing.

A single main loop in the kinetic Monte Carlo model can be summarized as follows.

- All possible transitions in the system, involving diffusion events from an occupied site into any unoccupied next-neighbor site, are identified and their corresponding transition rates are computed.
- A diffusion event is determined by randomly choosing from all the possible jumps weighted by their relative rate of occurrence given by equation (8).
- The transition is performed and the system is updated.

The Monte Carlo steps (MCS) time unit is defined such that $N_{\rm T}$ iterations of the preceding loop correspond to one MCS. In the kinetic Monte Carlo approach the connection between 'real time' and MCS time is established in the following way: let μ be a label for all possible transition events in the system. The transition rate $P_\mu = \nu_0 \exp(-\frac{E_\mu}{k_{\rm b}T})$ has the dimension of a frequency, and its reciprocal can be considered as the residence time for the particle involved in the transition. As transition probabilities for all possible events are independent, the overall probability per unit time for the system to perform a transition is obtained by adding all possible transition rates, namely $P = \sum_\mu P_\mu$. Therefore, $\frac{1}{P}$ is the mean residence time for the system in a specific state and, consequently, it represents the mean time associated with one iteration.

In this work we considered five different models for activation energies. The common feature in all this models is that the activation energy for a transition from the state $c_{\rm ini}$ to the state $c_{\rm fin}$ only depends on the energies of those states. We label these different activation energy models with the acronyms MARM, EINI, EINI-C, EAM-Ni and EAM-Cu, and these models are described as follows.

- MARM: In this model, a harmonic dependence of the energy as a function of the reaction degree is assumed. This model has been considered previously in KMC studies applied to surface diffusion of clusters [36, 37], and also in the same context as in the present paper [23]. The activation barriers are obtained simply by considering the crossing of two such harmonic potentials displaced a lattice-constant unit. A more detailed description of this harmonic model can be found in [23, 36, 37]. Here we shall restrict ourselves to give the final expression for the activation energy, namely

$$E^{\rm act}_{\rm ini\rightarrow fin} = \frac{\epsilon}{2}\left(\frac{E_{\rm fin} - E_{\rm ini}}{\epsilon} + \frac{1}{2}\right)^2, \qquad (9)$$

  where $E_{\rm ini}$ and $E_{\rm fin}$ are the energies of the initial and final states, respectively. Also we called $\epsilon = ka^2$, where k is the force constant of the harmonic wells and a is the lattice constant. Throughout this work, we have taken $a = 0.3$ nm and $\epsilon = 1$ eV. By performing a simple replacement in the Hamiltonian (7), the energy difference $E_{\rm fin} - E_{\rm ini}$ can be expressed in terms of the variation of the number of occupied neighbors (Δn) caused by a diffusing particle, i.e. $E_{\rm fin} - E_{\rm ini} = E_{\rm b}\Delta n$.
- EINI: Here activation energies only depend on the energy of the initial state $E^{\rm act} = -E_{\rm ini}$, irrespective of the final state. In spite of its simplicity, this model has frequently been considered in the literature, in contexts similar to that of the present paper [43–45].
- EINI-C: This model is a slight variation of the EINI model, since it has only an additional constraint. In fact, activation energies in the EINI-C model are obtained in the same way as in the EINI model, except for the case in which the particle trying to perform the movement attempts to make a transition from a state with a nonzero coordination number ($z \neq 0$) to a state with $z = 0$. Here, these kinds of transitions are forbidden. Thus, while particles can eventually detach from a given cluster in a single diffusion event in the EINI model, this can no longer occur in the EINI-C model. Nevertheless, it is important to notice that, even in the EINI-C model, a given particle with coordination number $z = 1$ can become uncoordinated ($z = 0$) if its unique nearest neighbor moves away from it, in a licit diffusion event.
- EAM-Ni and EAM-Cu: With these acronyms we refer to models in which the activation energies for all possible transitions (to first-neighbor paths) in two-dimensional triangular lattices are obtained by means of the embedded atom model (EAM) [46–49]. Activation energies for nickel (EAM-Ni) and copper (EAM-Cu) employed in this paper correspond to results that have previously been reported in the literature [50].

It is worth mentioning that, even by starting from a single-cluster configuration, one has a rich scenario of possible kinetic evolution. In fact, particles can evaporate from the cluster, voids can appear, new clusters, unconnected to the original one, can also grow during the dynamic evolution process, etc. In this way, a certain programing effort is necessary in order to distinguish between the main cluster (connected to the bottom of the system by a path of nearest neighbors) and other clusters in the system. Let $h_{\rm i}$ be the position of the highest occupied site at the ith column on the main cluster. We characterize the fluctuations of the interface by means of a standard estimator, such as the interface roughness, $(W(L_x, t))$, given by

$$W(L_x, t) = \sqrt{\frac{1}{L_x}\sum_{i=1}^{L_x}(h_{\rm i}(t) - \overline{h}(t))^2}, \qquad (10)$$

where $\overline{h}(t) = 1/L_x \sum_{i=1}^{L_x} h_{\rm i}(t)$. It is worth noticing that some results are presented by using nanometers (nm) as the length unit, while in other cases the use of lattice units is more convenient. In any case, it is a trivial task to switch between units: for lengths along the x axis one has to multiply the length in lattice units times the distance among closest neighbors in the triangular lattice a, which was taken as $a = 0.3$ nm for models MARM, ENI and EINI-C, while the value of a for models EAM-Ni and EAM-Cu was obtained from

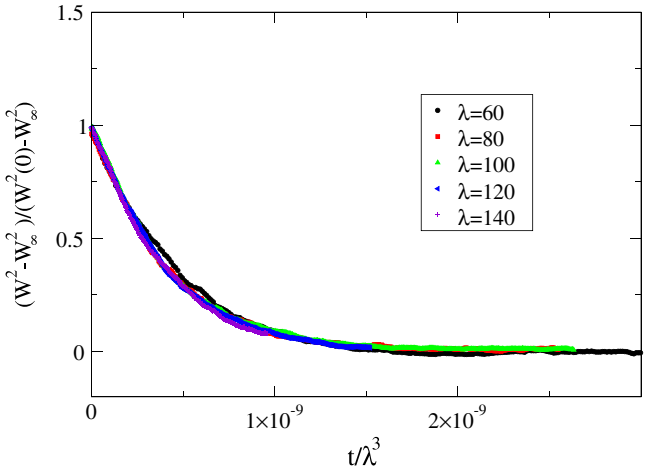

Figure 6. (Color online) Data collapse found for results corresponding to the model EINI when the squared roughness and the time axis are rescaled as is indicated in equation (13). Different λ values are indicated in lattice units and the simulation temperature was 300 K.

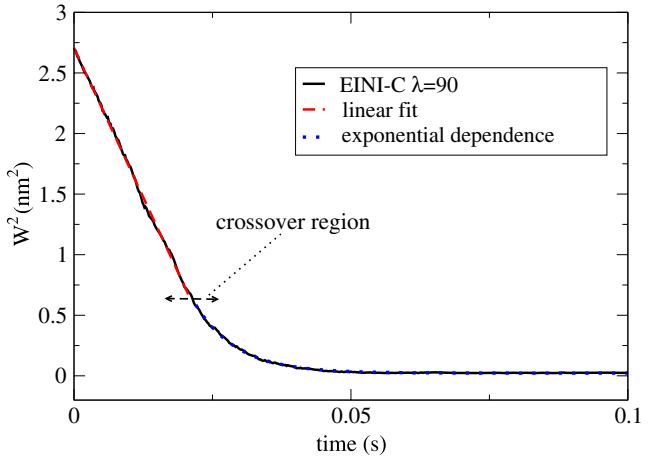

Figure 7. (Color online) Typical behavior found for the decay of W^2 as a function of time, in the case of the EINI-C model (actually, the same kind of behavior is also found for models EAM-Cu and EAM-Ni). A transition from a linear dependence to an exponential decay is clearly observed, and the transition takes place at a narrow crossover region. The parameters corresponding to this simulation are: $\lambda = 50$ (in lattice units), $T = 300$ K and simulation data are averaged over 50 independent runs.

the lattice units of their corresponding FCC structures. For distances along the y axis an additional factor $\frac{\sqrt{3}}{2}$ appears due to the geometry of the triangular lattice. While according to equation (4) the linear continuous theory of surface diffusion predicts a vanishing asymptotic interface roughness, discrete models such as the KMC models studied in this paper often have a nonvanishing asymptotic interface roughness W_∞ at nonzero temperatures, as a consequence of the internal noise that is always present in discrete systems [51]. Thus, we propose a direct generalization of the linear continuous theory result, in order to take into account the discrete nature of matter, regarding the prediction for the interface roughness evolution of a small-amplitude Fourier mode $A\sin(kx)$, given by

$$W^2(\lambda, t) = \frac{A^2}{2}\exp\left(-2Kk^4t\right) + W_\infty^2\left(1 - \exp\left(-2Kk^4t\right)\right). \tag{11}$$

Nevertheless, it has been found [24] that, although the MARM and ENII models both exhibit an exponential decay of W, while the MARM model has a power-law dependence of the decay constant $\kappa \sim \lambda^{-4}$, in complete agreement with equation (11), the corresponding exponent becomes 3 in the case of the EINI model. It is possible to perform a rescaling of the axes if we plot W against time in order to obtain data collapse of the curves corresponding to different values of λ. Nevertheless, due to the different exponents governing the power-law decay of κ with λ, by rescaling a single axis one cannot achieve data collapse for both MARM and EINI models simultaneously. So, that rescaling must be done independently. However, by rewriting equation (11) as

$$W^2(\lambda, t) = W^2(0)\exp\left(-2Kk^nt\right) + W_\infty^2\left(1 - \exp\left(-2Kk^nt\right)\right), \tag{12}$$

for an arbitrary exponent n, it becomes evident that we will be able to get data collapse after rearranging equation (12) as follows:

$$\frac{W^2(\lambda, t) - W_\infty^2}{W^2(0) - W_\infty^2} = \exp\left(-2Kk^nt\right). \tag{13}$$

By applying this procedure we obtained a quite good data collapse for the EINI model at 300 K, as shown in figure 6.

Although the generalization of the linear theory of surface diffusion provided by equation (11) shows a good agreement with KMC data for both the MARM and EINI models, this is not the case for the models EINI-C, EAM-Ni and EAM-Cu. For these models, a qualitatively different temporal evolution of the roughness was found: an initial linear decay of W^2 is followed, after a narrow crossover region, by an exponential decay. A typical curve for this kind of 'anomalous' roughness evolution is shown in figure 7. The plotted data correspond to a KMC simulation for the EAM-C model, and the best-fit curves for the initial (linear) and final (exponential) stages are also plotted. It is clear from figure 7 that this transition from a linear to an exponential decaying regime takes place in a very narrow crossover region, where both curves and numerical data merge smoothly together (see the double arrow in figure 7).

For initial sinusoidal profiles far from the small-slope approximation, we obtain a spontaneous overhang formation in the intermediate state, before the decay of the interface into the equilibrium nearly-flat shape. This can be observed in the typical snapshots (taken at $T = 300$ K for the MARM model) shown in figure 8, which correspond to the decay of a sinusoidal interface with $A = 20$ and $\lambda = 20$ (in lattice units) so that $\frac{A}{\lambda} \sim 1$. The shape of the interface at different stages is very similar to that found in the continuous model for the decay of sinusoidal profiles with initial aspect ratios near to 1, such as those sketched in figure 4(b) and described by the ansatz in equation (6). Of course, some differences also become evident due to the stochastic nature of the Monte Carlo model and some faceting that can be observed in the snapshots of figure 8.

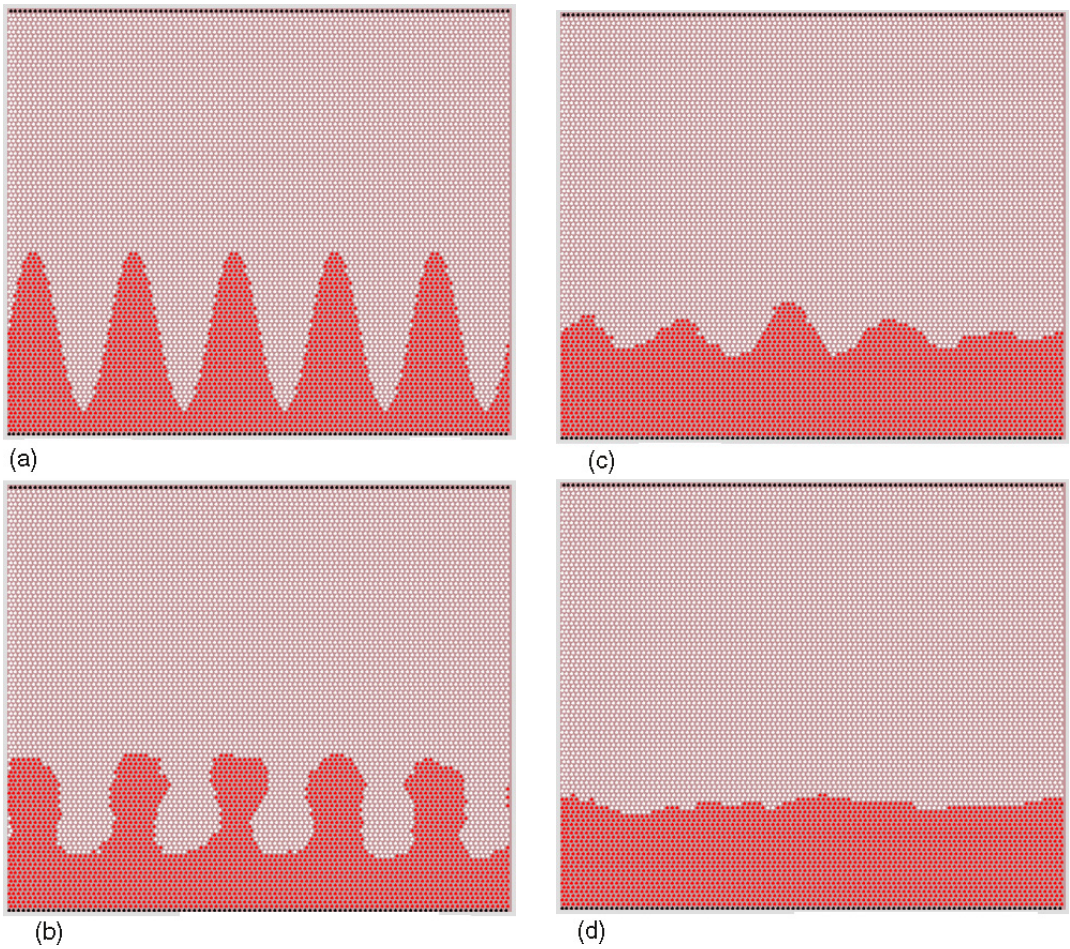

Figure 8. (Color online) (a) Initial condition, (b) 150 MCS, (c) 400 MCS, (d) 500 MCS. Snapshots of the interface at successive times (indicated in MCS) showing the decay of a initially sinusoidal profile far from the small-slope approximation. Simulated temperature is $T = 300$ K and geometrical parameters in the initial wave are (in lattice units) $A = 20$ and $\lambda = 20$. The activation energy model used in the simulation is the MARM.

Varying the temperature in a rather large range does not change this behavior. Moreover, it is important to notice that this result, from a qualitative point of view, does not change when we change the activation energy model considered, since the same morphologic behavior shown for the MARM model in figure 8 has been obtained for models EINI, EINI-C, EAM-Ni and EAM-Cu [24].

Let us present some typical results on the time evolution of initially rectangular patterns. Let B_s and B_i be the upper and lower basis of the pattern and H the height of the rectangles. The spatial period of the pattern then is $B_s + B_i$. More specifically, we are interested in the relaxation behavior of patterns in the large-slope case (i.e. for $H \geqslant B_s, B_i$) and varying the ratio between the bases B_s and B_i.

In the case in which $B_s \ll B_i$, the rectangular features are unstable and after a short transient every rectangle in the pattern breaks off into several islands, the number of such islands being a stochastic quantity, with an average proportional to the height of the rectangles H. The average size of the islands is also proportional to the width of the rectangles B_s. In this way, the transient state is conformed by a number of small clusters arranged in a matrix-like structure, as can be seen in figure 9. This breaking off of nanostructures may be relevant if we consider the following situation: a metallic contact supported on an insulator substrate. Depending on the surface mobility and on geometrical parameters of the nanocontact, this may break off by surface diffusion and the system turns out into an insulator. This effect can be seen in figure 10, where an initial bridge-like structure (figure 10(a)) turns out unconnected due to surface diffusion.

If we consider an initial rectangular pattern in which $B_i \ll B_s$, fluctuations on the sides of adjacent rectangles cause them to merge, forming voids. The situation is closely related to the case of the emergence of nanoislands, and it can be thought as some kind of island–void symmetry, since both are complementary to a certain degree: the average size of the nanovoids is proportional to B_i, while the average number of voids formed between two rectangles is proportional to H. The whole picture is that of a matrix-like arrangement of nanovoids appearing after a short transient, as is shown in figure 11.

It is important to stress that the exposed morphological results in figures 8–11, are not dependent on the particular activation energy model choose. Thus, the reported morphological stages have a much more universal character

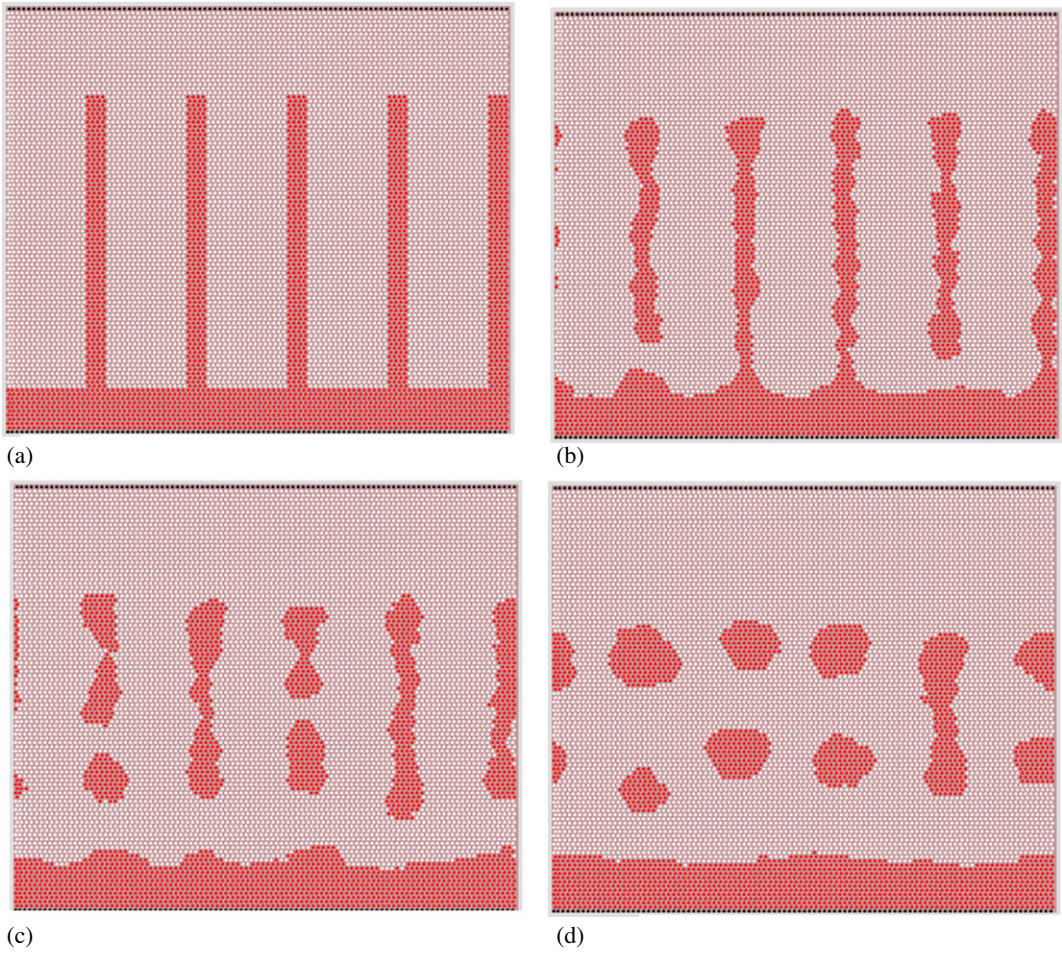

Figure 9. (Color online) (a) Initial condition, (b) 50 MCS, (c) 150 MCS, (d) 500 MCS. Snapshots at successive times (indicated in MCS) showing the decay of a rectangular pattern in the case $B_s \ll B_i$ for the model MARM. A transient state consisting of a matrix-like array of nanoislands is clearly observed. Temperature in the simulation is 300 K, and geometrical parameters of the initial pattern are (in lattice units) $H = 70$, $B_s = 4$ and $B_i = 16$.

than kinetic properties, that, as we discuss above, are model-dependent. For instance, in figure 12 we compare snapshots of the five activation energy models considered in this work, starting from a same initial rectangular profile with $B_i = B_s$. It is evident that the morphological structures formed are very similar, independently of the activation energy model considered. Furthermore, as is shown in figure 12, for all the models we also found that an initially rectangular profile develops patterns that are very similar to those shown in figure 8(b). This finding means that in all cases a fast filtering of high-frequency modes operates, so that 'memory' effects on the initial rectangular profile are lost and the systems evolve in the same way as if they were started from a sinusoidal (lowest-frequency Fourier mode) profile. As was pointed out in [23], it is interesting to notice that such high-frequency filtering takes place under a clearly nonlinear regime, in which superposition-principle ideas are *a priori* no longer applicable. Of course, the snapshots of figure 12 were taken at different MCS, which is understable since, as we have pointed out above, kinetic properties strongly depend not only on temperature but also on the model considered for activation energies.

5. Summary and concluding remarks

We have reviewed recent results concerning the decay of two-dimensional nanostructures driven by surface diffusion currents. Both continuous and discrete modeling of the same phenomenon were discussed and compared. From the point of view of continuous modeling, a vectorial scheme to integrate numerically a flow in which the normal velocity is proportional to the intrinsic Laplacian of the local curvature was followed. In addition, kinetic Monte Carlo simulations of two-dimensional models for the study of nanostructure decay were reviewed. Different alternatives for the activation energies associated with diffusion paths, including a harmonic model (MARM), models only sensitive to the energy of the initial state of the diffusing particle (EINI and EINI-C), and also models where activation energies were obtained by means of the embedded atom model (EAM-Ni and EAM-Cu) have been considered. The study of both kinetic properties of the decay of sinusoidal profiles within the small-slope approximation, and morphological properties related to the decay of high-aspect-ratio structures was considered. The results were compared not only among the different activation

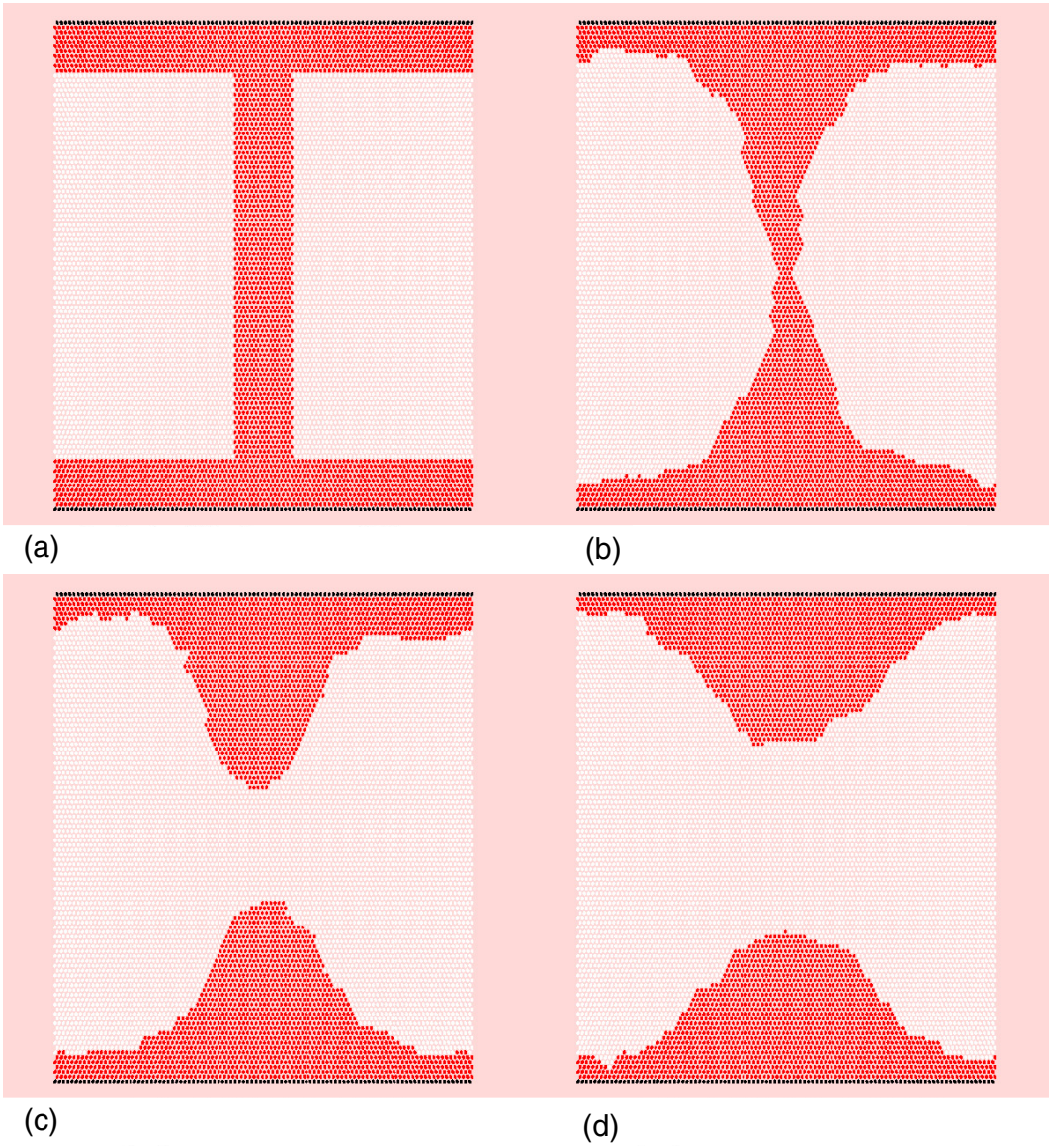

Figure 10. (Color online) (a) Initial condition, (b) 7000 MCS, (c) 8000 MCS, (d) 10 000 MCS. An initial bridge-like structure breaks off, turning out unconnected due to surface diffusion currents. Simulated temperature is 300 K and the activation energy model used is the MARM.

energy models used, but also with the predictions from the continuous modeling.

Results from the continuous modeling show that predictions from the linear theory of surface diffusion were recovered in the case of interfaces under the small-slopes approximation. Moreover, in the general case, simulations show nonexponential decaying modes and spontaneous overhang generation.

Concerning kinetic properties of the discrete modeling, we found that, for the decay of small-amplitude sine-like profiles, in the case of the MARM and EINI models, the interface roughness follows a displaced-exponential dependence, which can be considered as a natural generalization of the continuous theory. Nevertheless, we also found that for the remaining models considered (i.e. EINI-C, EAM-Ni and EAM-Cu) the interface roughness follows a qualitatively different time decay evolution, since it is linear during an initial stage and, after a short crossover region, it becomes exponential. Although the decay–lifetime dependence on the profile wavelength follows power laws in all cases, the associated exponent is model-dependent.

Concerning the morphological properties of high-aspect-ratio pattern decay, we found that shape evolution is qualitatively similar irrespective of the particular activation energy model used and, even more remarkably, this evolution is quite similar to that predicted by the continuous theory of surface diffusion. In particular, sinusoidal profiles of initial aspect ratios of the order of 1 (i.e. far from the small-slopes approximation) show the spontaneous development of overhangs during a transient stage, and the interface shape can approximately be described by the ansatz given by equation (6). In the case of very narrow rectangular slabs ($B_s \ll B_i \leqslant H$), rectangles break down into several nanoislands during a transient regime. Although the number

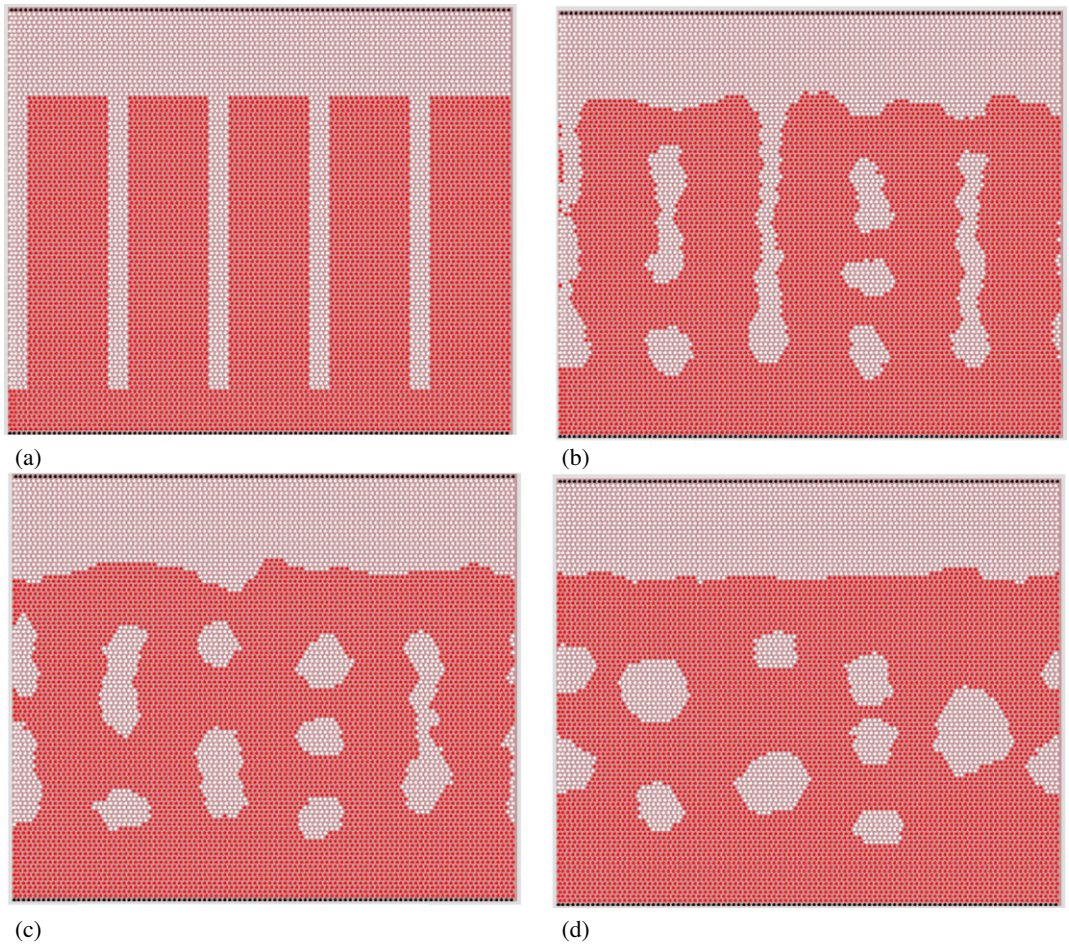

Figure 11. (Color online) (a) Initial condition, (b) 50 MCS, (c) 100 MCS, (d) 500 MCS. Snapshots at successive times (indicated in MCS) showing the decay of a rectangular pattern in the case $B_i \ll B_s$ for the model MARM. The formation of a transient state consisting of a matrix-like array of nanovoids is evident. Temperature in the simulation is 300 K, and geometrical parameters of the initial pattern are (in lattice units) $H = 70$, $B_s = 16$ and $B_i = 4$.

and size of such nanoislands depend on kinetic aspects, such as the particular activation energy model, from a morphological point of view, we found that this transient regime is observed in all cases and it looks qualitatively similar, irrespective of the activation energy model considered. Similarly, a rectangular array of voids, in the transient stage, was found in the case $B_s \gg B_i \leqslant H$.

Kinetic properties of nanopattern decay strongly depend on the activation energy model considered. In this sense, kinetic predictions from the continuous theory of surface diffusion are expected to be in agreement with the observation of the actual evolution of a discrete system, only in some particular cases. In contrast, continuous theory predictions concerning morphological aspects show a wider applicability. In fact, that theory describes, in a qualitatively correct way, the observed morphologies in a wide range of situations and irrespective of the activation energy model considered. In this way, we expect that this work will contribute to stimulate experimental research in this field aimed to test, in real nanotechnological systems, the predictions of the continuous surface diffusion theory concerning morphological aspects.

These results have shown that, for both the discrete kinetic Monte Carlo approach and the continuum description, overhang formation during the intermediate stages of the equilibration process is quite frequent, becoming the rule rather than the exception. In this sense, we stress the importance of modeling this kind of system in a way that accounts for the possible formation of overhangs during the dynamic evolution. In contrast, highly restrictive models like standard solid-on-solid models [34], which by definition do not allow for overhangs, cannot describe either multi-valued interfaces and void formation or other interesting physical situations. Thus, the discussed results should be taken into account in future work, in order to develop models relevant to nanotechnological systems having enough flexibility to describe those situations.

In this work we have reviewed recent results in which theoretical results, continuous modeling and discrete kinetic Monte Carlo simulations were extensively compared and complemented. This complementarity among very different modeling strategies has its own theoretical relevance because the relationship between continuous descriptions and discrete models is still under debate in several physical situations, such as the theory of evolving interfaces in growing models [34]. It is worth mentioning that, by identifying the correct model capable of describing an actual physical system,

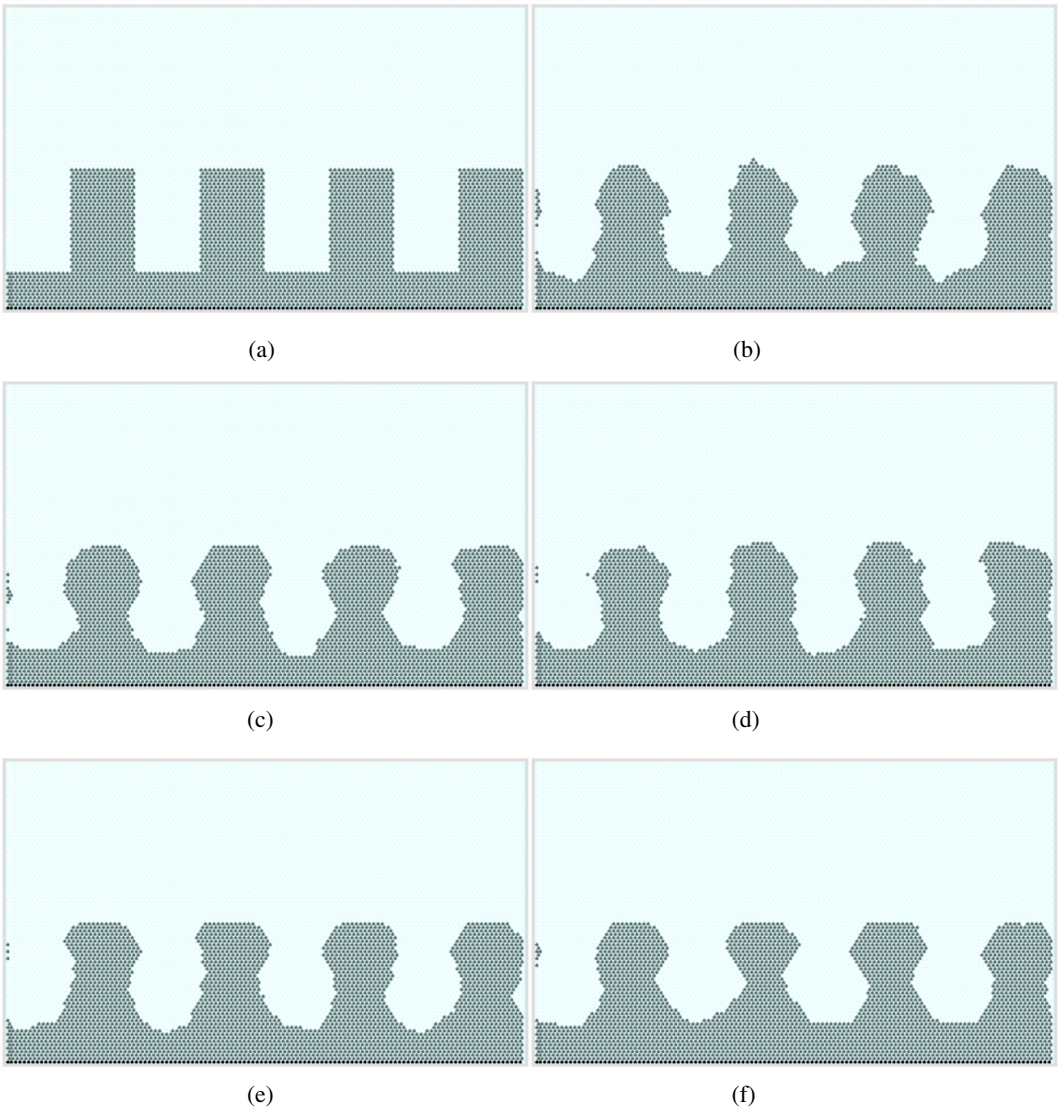

Figure 12. (Color online) System evolution for each model considered starting from the same initial rectangular profile shown in (a), after the number of MCS indicated in each snapshot. (b) Model MARM at 100 MCS and at $T = 300$ K. (c) Model EINI-C at 1000 MCS and at $T = 300$ K. (d) Model EINI at 400 MCS and at $T = 300$ K. (e) Model EAM-Cu at 4000 MCS and at $T = 800$ K. (f) Model EAM-Ni at 100 MCS and at $T = 800$ K. The geometrical parameters of the initial rectangular pattern are $B_i = 15$, $B_s = 15$ and $H = 30$, all of them measured in lattice units.

computer simulations can become a powerful tool aiding the nonexpensive design of nanodevices and nanopatterns.

Acknowledgments

This work has been performed as part of the projects PICT 06-621 and PICT 06-36 of ANPCyT (Argentina). The authors are members of CONICET (Argentina National Research Council) and UNLP.

References

[1] Bales G S, Redfield A C and Zangwill A 1989 *Phys. Rev. Lett.* **62** 776
[2] Karunasiri R P U, Bruinsma R and Rudnick J 1989 *Phys. Rev. Lett.* **62** 788
[3] Israeli N and Kandel D 1998 *Phys. Rev. Lett.* **80** 3300
[4] Kallabis H and Wolf D E 1997 *Phys. Rev. Lett.* **79** 4854
[5] Fu E S, Johnson M D, Liu D J, Weeks J D and Williams E D 1996 *Phys. Rev. Lett.* **77** 1091
[6] Erlebacher J, Aziz M J, Chason E, Sinclair M B and Floro J A 2000 *Phys. Rev. Lett.* **84** 5800
[7] Dubson M A and Jeffers A 1994 *Phys. Rev.* B **49** 8347
[8] Maritan A, Toigo F, Koplic J and Banavar J R 1992 *Phys. Rev. Lett.* **69** 3193
[9] Son C-S, Kim T, Wang X-L and Ogura M 2000 *J. Cryst. Growth* **221** 201
[10] Murty M V R 2000 *Phys. Rev.* B **62** 17004
[11] Israeli N and Kandel D 2002 *Phys. Rev. Lett.* **88** 116103
[12] Kan H C, Shah S, Tadyyon-Eslami T and Phaneuf R J 2004 *Phys. Rev. Lett.* **92** 146101
[13] Bonzel H P and Latta E E 1978 *Surf. Sci.* **76** 275
[14] Bonzel H P and Preuss E 1995 *Surf. Sci.* **336** 209
[15] Giesen-Seibert M, Jentjens R, Poensgen M and Ibach H 1993 *Phys. Rev. Lett.* **71** 3521

[16] Giesen-Seibert M and Ibach H 1994 *Surf. Sci.* **316** 205
[17] Timp G L 1999 *Nanotechnology* (New York: Springer)
[18] Kolb M, Ullmann R and Will T 1997 *Science* **275** 1097
[19] Rieth M 2003 *Nano-Engineering in Science and Technology* (Singapore: World Scientific)
[20] Andreasen G, Schilardi P L, Azzaroni O and Salvarezza R C 2002 *Langmuir* **18** 10430
[21] Castez M F, Fonticelli M H, Azzaroni O, Salvarezza R C and Solari H G 2005 *Appl. Phys. Lett.* **87** 123104
[22] Castez M F, Salvarezza R C and Solari H G 2006 *Phys. Rev.* E **73** 011607
[23] Castez M F and Albano E V 2007 *J. Phys. Chem.* C **111** 4606
[24] Castez M F and Albano E V 2008 *Phys. Rev.* E **78** 031601
[25] Mullins W W 1957 *J. Appl. Phys.* **28** 333
[26] Mullins W W 1959 *J. Appl. Phys.* **30** 77
[27] Herring C 1951 *Physics of Powder Metallurgy* ed W E Kingston (New York: McGraw-Hill)
[28] Herring C 1952 *Structure and Properties of Solid Surfaces* ed R Gomer and C S Smith (Chicago: The University of Chicago Press)
[29] Lapujoulade J 1994 *Surf. Sci. Rep.* **20** 191
[30] Mayer U F 2001 *Comput. Appl. Math.* **20** 361
[31] Wolf D E and Villain J 1990 *Europhys. Lett.* **13** 389
[32] Sarma S D and Tamborenea P 1991 *Phys. Rev. Lett.* **66** 325
[33] Lai Z W and Sarma S D 1991 *Phys. Rev. Lett.* **66** 2348
[34] Barabasi A L and Stanley H E 1995 *Fractal Concepts in Surface Growth* (Cambridge: Cambridge University Press)
[35] Hecht E and Zajac A 1974 *Optics* (Reading, MA: Addison-Wesley)
[36] Kang H C and Weinberg W H 1988 *Phys. Rev.* B **38** 11543
[37] Kang H C and Weinberg W H 1989 *J. Chem. Phys.* **90** 2824
[38] Fichthorn K A and Weinberg W H 1991 *J. Chem. Phys.* **95** 1090
[39] Metropolis N, Rosenbluth A W, Rosenbluth M N, Teller A H and Teller E 1953 *J. Chem. Phys.* **21** 1087
[40] Glauber R J 1963 *J. Math. Phys.* **4** 294
[41] Kawasaki K 1972 *Phase Transitions and Critical Phenomena* vol 2, ed C Domb and M S Green (New York: Academic)
[42] Heermann D W 1989 *Computer Simulation Methods* (Heidelberg: Springer)
[43] Combe N, Jensen P and Pimpinelli A 2000 *Phys. Rev. Lett.* **85** 110
[44] Combe N and Larralde H 2000 *Phys. Rev.* B **62** 16074
[45] Iguain J L and Lewis L J 2003 *Phys. Rev.* B **68** 195407
[46] Daw M S and Baskes M I 1983 *Phys. Rev. Lett.* **50** 1285
[47] Daw M S and Baskes M I 1984 *Phys. Rev.* B **29** 6443
[48] Johnson R A 1988 *Phys. Rev.* B **37** 3924
[49] Yang Y G, Johnson R A and Wadley H N G 1997 *Acta Mater.* **45** 1455
[50] Yang Y 2000 *PhD Thesis* University of Virginia, advisor: H N G Wadley
[51] Kampen N G V 1992 *Stochastic Processes in Physics and Chemistry* (Amsterdam: Elsevier)